Viser Technology Pte. Ltd.
Mechanical Engineering Science
DOI: 10.33142/mes.v3i2.6724

Research Article Open Access

Aerothermodynamic Design and Flow Characteristics for a S-CO_2 Radial Inflow Turbine

Lehao HU[1], Yu JIANG[1], Qinghua DENG[1, 2, *], Zhuobin ZHAO[1], Jun LI[1, 2], Zhenping FENG[1]

1 Institute of Turbomachinery, Xi'an Jiaotong University, Xi'an, China
2 Collaboration Innovation Center of Advanced Aeroengine, Beihang University, Beijing 100191, China

***Corresponding Author:** Qinghua DENG, No. 28, Xianning West Road, Xi'an 710049, Shaanxi Province, China; qhdeng@mail.xjtu.edu.cn*

Abstract:
In this paper, a radial inflow turbine is designed for the 150 kW S-CO_2 Brayton cycle system, and flow characteristics and off-design performances are analyzed. The design results are accurate and high performances can be achieved for the S-CO_2 power system, and the total-static efficiency of 86% and net output power about 285.2 kW can meet the design requirements of S-CO_2 cycle system. The results of the flow characteristics show the streamlines of radial inflow turbine distribute uniformly, and the vortexes generated at the shroud of the blade suction surface have little influence on the turbine performances. The off-design performances show the total-static efficiency remains above 80% in the pressure ratio range of 1.6 ～ 2.9, and the output power and mass flow rate increase with the pressure ratio increasing. It is indicated that the designed turbine has excellent off-design performances and can meet the operation requirements. The study results can provide guidance for S-CO_2 radial inflow turbine design and operation.
***Keywords:** supercritical carbon dioxide; radial inflow turbine; flow characteristics; off-design performances*

1 Introduction

A power cycle is a collection of the process and machinery used to generate useful energy such as power energy and mechanical energy from heat sources. There are lots of different power cycles, and the most commonly used for large-scale power generation are Brayton cycle, in which a single-phase gas is in the complete cycle, and Rankine cycle where there is a transition between vapor and liquid phases. In 1968, Angelino [1] and Feher [2] proposed that a supercritical fluid operating in supercritical region, never crossing into the gas-liquid two-phase region, serves as the working fluid of a power cycle. A number of researches have shown that the selection of supercritical carbon dioxide (S-CO_2) as the working fluid for a power cycle can increase the cycle efficiency by making full use of the special physical properties near the critical point, and allow the cycle system to be combined with a wide range of heat sources and the variations of the cycle to be operated with heat rejection to near-ambient sinks due to a nearly ambient critical temperature (31℃) for CO_2.

In addition, the Brayton cycle using S-CO_2 as the working fluid has the potential to attain significantly higher cycle efficiency than either the air Brayton cycle or the steam Rankine cycle, and there is a possibility for the S-CO_2 turbomachinery to be smaller than those of other power cycles due to the relatively high density of S-CO_2 [3]. The efficiency of 50% for S-CO_2 Brayton cycle is greatly larger than that of the ultra-supercritical steam Rankine cycle [4]. The size of component including turbine and compressor employed S-CO_2. Brayton cycle is one fifth as that of turbomachinery used other working fluids such as helium gas at same output power [5]. The results in Ref. [6] have shown that the aerothermal performances of the turbomachinery have the significantly influence on the S-CO_2 Brayton cycle system, and the turbine may be the most complicate component for entire cycle system due to a lack of design experience.

Perhaps the most widely known S-CO_2 turbine designed by Wright et al. [7] was installed in S-CO_2 Brayton cycle loop at Sandia National Laboratory. The designed rotation speed and impeller diameter of the turbine are 75, 000 r/min and 68.1 mm, respectively. The operation indicated that the high density and low viscosity of S-CO_2 have led to fouling, which also results in significant erosion in turbine nozzles [8-9]. The test loop for S-CO_2 Brayton cycle was constructed at Bettis Atomic Power Laboratory to verify the cycle efficiency predicted by theoretical method and investigate the operation characteristics of turbomachinery [10-13]. At inlet of tested turbine that can generate the power energy of 100 kW, temperature and pressure of S-CO_2 are 299 ℃ and 16.3 MPa. However, the cycle efficiency of 7.5% is

Received on October 24, 2021; Accepted on December 23, 2021

far less than that for large-power S-CO_2 Brayton cycle since the greatly larger relative clearance formed stationary component and rotating impeller results in larger leakage flow loss and windage loss. The radial inflow turbine applied to 10 kW scale S-CO_2 Brayton cycle test loop was designed and constructed by Cho et al. [14-17]. The working fluid of 3.04 kg/s can pass through turbine that extract work of 82.4 kW when temperature and pressure at inlet are 453 K and 13 MPa. Considering extremely high rotation speed, the closed impeller is more reasonable comparing to opened impeller because of significantly small blade height and greatly large pressure of S-CO_2. In addition, the numerous scholars including Cho working at Korea Energy Research Institute designed the two different power S-CO_2 Brayton cycles to validate the feasippbility of cycle principle and machined a radial inflow turbine to generate the power. Zhou et al. [18] introduced a design method aimed at radial inflow turbine, designed a 1.5 MW S-CO_2 radial inflow turbine by using the self-programming software and analyzed the flow characteristics based on the numerical study.

The 450 MW S-CO_2 Brayton cycle system with reheat and recompression used for a coal fired power plant was designed and operated by General Electrics Company [19-20]. Based on the cycle, the high-pressure and low-pressure axial turbines whose rotation speed is 3,600 r/min are designed. The working fluid of total temperature of 973.15 K and total pressure of 25.06 MPa at inlet of the high-pressure turbine having four-stage is able to transform the heat energy of 90.6% to mechanical energy, and total-static efficiency of the three-stage low-pressure turbine attains 91.6% while total temperature and total pressure are 953.15 K and 12.96 MPa at inlet. The working fluid passes through the high-pressure and low-pressure turbines from the opposite direction, which decreases significantly the axial thrust and makes turbine operation easier. The blade height of the first-stage and third-stage of the high-pressure turbine are only 71.12 mm 137.16 mm, which is far lower than that of the steam turbine for same power scale turbine.

In this paper, the radial inflow turbine is designed for a 150 kW S-CO_2 Brayton cycle based on the self-programming code, and flow characteristics under design condition and performances under off-design conditions are analyzed by the numerical investigation. The study results can provide the guidance for S-CO_2 radial inflow turbine design and operation [21].

2 Design of S-CO_2 Radial Inflow Turbine

2.1 Aerothermodynamic design of radial inflow turbine

The radial inflow turbine whose performances have a direct influence on cycle efficiency is an important component extracting work from the heat sources. Based on 150 kW S-CO_2 Brayton cycle system composed of the compressor, recuperator, heater, turbine, generator and cooler as shown in Figure 1, design parameters of S-CO_2 turbine are able to be obtained and listed in Table 1. It is worth mentioning that the value of mass flow rate listed in Table 1 for practical design process is about increased to 125% as that shown in Figure 1 required by S-CO_2 Brayton cycle, which ensures that the whole cycle could loop smoothly to avoid unknown losses in main parts and make the output power meet the requirements. Therefore, the mass flow rate is determined as 3.61 kg/s as listed in Table 1. At the moment, it is noted that the values of pressure drop are determined by referring to the S-CO_2 Brayton cycle designed by Sandia National Laboratory. They assumed that the pressure drops for cooler and regenerator at low temperature side are about 0.8% of pressure at compressor inlet, and that of heater and regenerator at high temperature side is 0.8% of pressure at compressor outlet. Therefore, the pressure drop value of cooler and regenerator at low temperature side is set as 65 kPa, and that of heater and regenerator at high temperature side is assumed as 130 kPa in this paper.

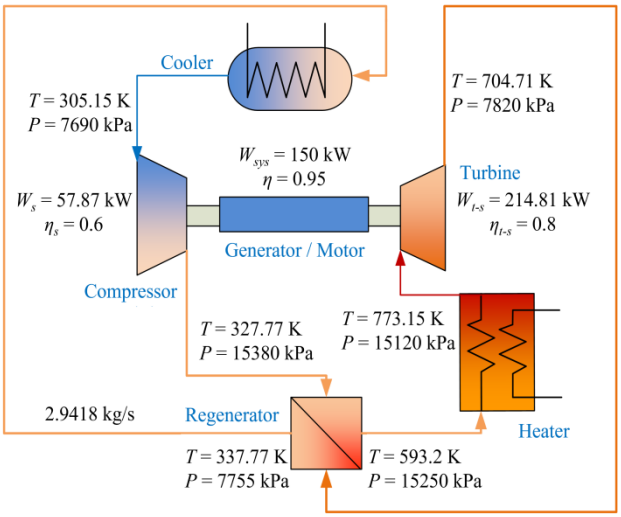

Figure 1 150 kW S-CO_2 Brayton cycle system

The aerothermodynamic design of the radial inflow turbine is based on self-programming code which has been developed and improved by choosing the appropriate loss model [22-23] in order to ensure the results accuracy, and Figure 2 shows flow chart for turbine design. For this program, the total-static efficiency $\eta_{t\text{-}s}$, geometric parameters of turbine and flow parameters of working fluid can be calculated by selecting a set of the load coefficient ψ, flow coefficient Φ and rotational speed n combined with design parameters listed in Table 1. In order to attain the highest total-static efficiency $\eta_{t\text{-}s}$ for a turbine, genetic algorithm is introduced to this program to seek out an optimum setting about ψ, Φ and n. In addition, considering variation of physical properties of CO_2 near or above critical point, the physical properties of the working fluid in this program come from REFPROP 9.0, which is real fluid property database developed by the National Institute of Standards and Technology (NIST). This program has been validated by the reference results to ensure its reasonability and accuracy, and it is also able to be used in the aerothermodynamic design process to achieve high performance for the S-CO_2 radial inflow turbine.

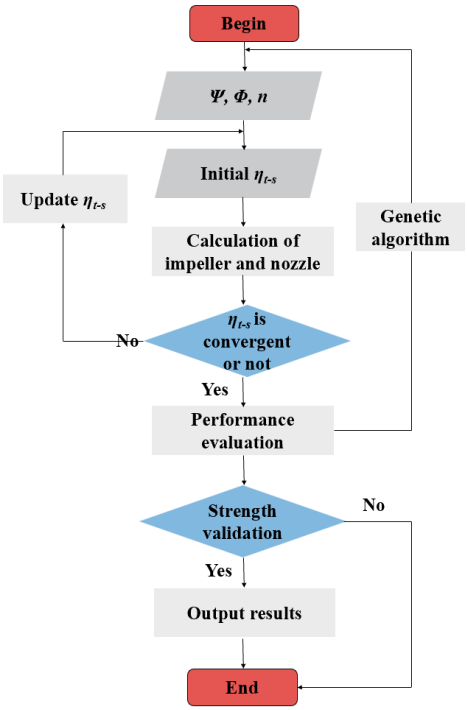

Figure 2 Flow chart of turbine design program

According to the design parameters listed Table 1 and the self-programming code, the geometric and flow parameters of S-CO_2 turbine are obtained and listed in Table 2. Total-static efficiency of 86% is larger than required that of 80%, and net output power about 285.2 kW also meet the design requirements of cycle system. However, it needs to be noted that absolute flow angle at impeller inlet α_1 of 8° is smaller than recommended value based on design experience aimed other working fluid turbine. This is because the relatively large S-CO_2 density at impeller inlet makes the blade height smaller if the recommended flow angle is adopted, which results in increasing flow leakage loss and raising the operation difficulty. The velocity triangle for the designed turbine is presented in Figure 3. Generally, the tip clearance value is depended on impeller blade height of 1% ～ 2% referring to conventional turbine. However, the shroud clearance referring to conventional turbine standard is too small to manufacture impeller blade, thus the value of 0.25 mm is finally determined.

In Figure 3, the subscripts "1" and "2" denote inlet and exit positions of the impeller, respectively. α, β denote absolute and relative flow angle, and C, W, and U denote absolute velocity, relative velocity and tangential velocity, respectively.

Table 1 Design parameters of S-CO_2 turbine

Design parameters	Value
Total temperature at turbine inlet / K	773.15
Total pressure at turbine inlet / MPa	15.12
Static pressure at turbine outlet / MPa	7.82
Mass flow rate / kg s^{-1}	3.61
Total-static efficiency	＞ 80%

Table 2 Design results of S-CO_2 radial inflow turbine

Parameters	Value
Rotation speed / r min^{-1}	60,000
Absolute flow angle at nozzle outlet / °	8
Absolute velocity at nozzle outlet / m s^{-1}	283.59
Blade height of nozzle / mm	3.89
Diameter of at nozzle inlet / mm	114
Diameter of at impeller inlet / mm	93.34
Relative velocity at impeller inlet / m s^{-1}	41.37
Relative flow angle at impeller inlet / °	107.45
Blade height at impeller inlet / mm	3.89
Relative velocity at impeller outlet / m s^{-1}	110.4
Relative flow angle at impeller outlet / °	24.46
Absolute velocity at impeller outlet / m s^{-1}	51.05
Absolute flow angle at impeller outlet / °	102.53
Hub diameter at impeller outlet / mm	20
Shroud diameter at impeller outlet / mm	45.4
Blade height at impeller outlet / mm	12.7
Shroud clearance / mm	0.25
Number of nozzle blade	15
Number of impeller blade	13
Total-static efficiency / %	86.0
Net output power / kW	285.2

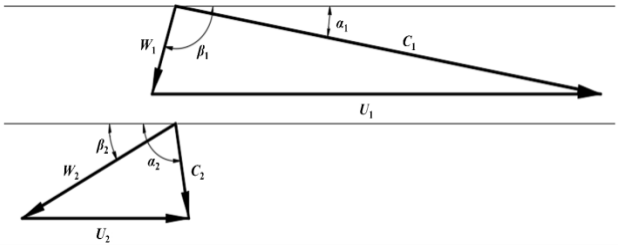

Figure 3 Velocity triangle for S-CO_2 radial inflow turbine

2.2 Blade geometric design

Figure 4(a) shows the meridional passage of S-CO_2 radial inflow turbine according to the parameters as shown in Table 2. In addition, the nozzle plays the major role on transferring the heat energy to kinetic energy and controlling the flow direction so that working fluid can flow smoothly into impeller based on the designed flow angle and fluid expands and extracts work. In this paper, nozzle blade profiles are designed referring to the island-type nozzle blade and the three-dimension geometry is shown in Figure 4(b).

The Non-Uniform Rational B-Splines method is used to design impeller blade profiles. The process of impeller blade design is performed by using the commercial software NUMECA Autoblade. After obtaining the profiles data, the three-dimension geometry is generated as presented in Figure 4(c). In addition, the designed S-CO_2 turbine composed of nozzle and impeller can be used to conduct the investigation of flow characteristics and analysis of the off-design performances.

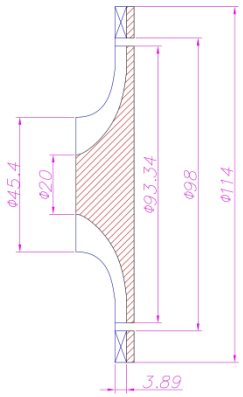

(a) Meridional passage

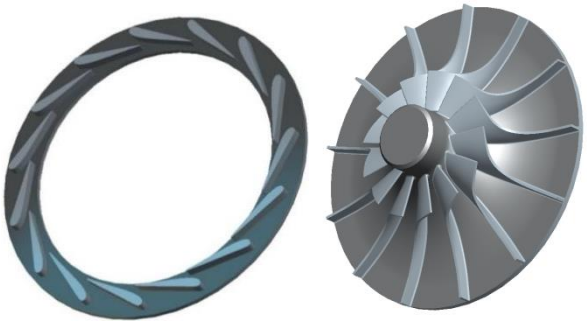

(b) Nozzle (c) Impeller

Figure 4 Schematic diagram of meridional passage and geometry

3 Numerical Method

In this paper, four kinds of turbulence model including Spalart-Almaras (S-A), k-ε, SST and k-ω are validated for the numerical method, and the results of total-static efficiency, output power and mass flow rate are listed in Table 3.

Table 3 Comparison of numerical results for the four turbulence models

Turbulence model	Total-static efficiency / %	Output power / kW	Mass flow rate / kg s^{-1}
S-A	86.00	284.24	3.606
k-ε	86.23	285.39	3.612
SST	86.87	286.32	3.597
k-ω	85.72	284.25	3.619

It is worth noting that there is a few of experimental data for S-CO_2 radial inflow turbine to this day, but no detailed geometry is published together with the performance results. So the results of four turbulence models here are only able to compare with themselves in this paper. As shown in Table 3, the deviations of four turbulence models are so low that the difference on the turbine performances can be ignored. Considering the time cost, S-A model is also most suitable among the four turbulence models. In addition, referring to the paper published by Jiang [24] and Zhang et al. [25], S-A model is often greatly applicable to simulate flow and analyze performances for axial or radial turbomachinery. Therefore, S-A model is reliable to investigate the flow in this paper.

For computational domain of the designed S-CO_2 turbine, mesh with default grid structure is obtained by the commercial software NUMECA Autogrid. Considering the adaptability of flow characteristics in boundary layer, mesh is denser at near-wall, endwall, leading edge, and trailing edge of nozzle and impeller blade. In addition, in order to ensure to meet the requirements of S-A turbulence model, the first cell height on the walls is 4.0×10^{-4} mm so that maximum Y^+ and averaged Y^+ are less than the order of unity. Figure 5 presents the computational domain mesh.

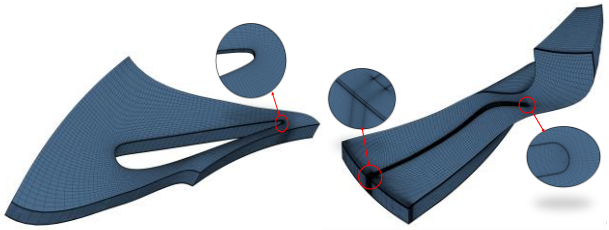

(a) Nozzle (b) Impeller

Figure 5 Mesh of S-CO_2 radial inflow turbine

To investigate accurately flow characteristics, Navier-Stokes equations are solved by using commercial software NUMECA FineTurbo. The four-step Runge-Kutta algorithm is adopted to ensure numerical time integration, and multigrid method is applied in order to decrease the solution time. In order to ensure that the working fluid can flow smoothly into the nozzle and flow out the impeller with no backflow and no vortexes, the extension section is set in front of the nozzle inlet and behind the impeller outlet. During whole computation process, mass flow rate at nozzle inlet and impeller outlet are monitored evaluating the stability of numerical simulation. When mass flow rate reaches to a stable value, less than 1% with additional iterations, simulation results are regarded as a "steady" state. In addition, the convergence of solution is attained with residual values at least below 1.0×10^{-5}. In all computational cases, there are no stability and convergence problems and every simulation typically requires 3,000 iterations.

The boundary conditions are set referring to the design parameters, total inlet pressure of 15.12 MPa, total inlet temperature of 773.15 K, and the flow angle of 45 ° at turbine inlet are set. The static pressure of 7.82 MPa is defined as the boundary condition at the turbine outlet. The rotational speed of the turbine impeller is set to be 60,000 r/min. The non-slip adiabatic wall is set for all walls including the endwall, which is consistent with the physical condition of the S-CO_2 turbine. Similarly, the physical properties of S-CO_2 are from real fluid property database developed by the NIST to ensure the accuracy of numerical simulation.

In order to ensure that the numerical simulation results are independent of grid number, a comparative study has been conducted with three kinds of different meshes of 1.0 million, 1.4 million, 2.0 million, and 3.0 million grids. For each grid, total-static efficiency, output power, and mass flow rate are listed in Table 4 for the design condition. It is seen that the relative deviation of

total-static efficiency for the mesh between 1.0 million grids and 1.4 million grids is 0.16%. With grids increasing to 2.0 million and 3.0 million, the range of relative deviation is 0.04% ～ 0.05%, which indicates that the 1.4 million grids can achieve grid-independent solution.

Table 4 Comparison of numerical results for different meshes

Grid number / M	Total-static efficiency / %	Output power / kW	Mass flow rate / kg s^{-1}
1.0	86.16	284.15	3.598
1.4	86.00	284.24	3.606
2.0	85.97	283.99	3.604
3.0	85.92	284.38	3.611

4 Results and Discussion

4.1 Flow characteristics under the design condition

The static pressure distribution and streamlines in meridional passage for S-CO_2 radial inflow turbine under design condition are presented in Figure 6 and Figure 7, respectively. From Figure 6 and Figure 7, it is seen that static pressure decreases along the flow direction, and there is no static pressure mutation due to no backflow and boundary layer separation near wall for the meridional passage, which indicates that the meridian passage design is reasonable. The averaged flow parameters in the meridional passage are only used to evaluate whole performance of the S-CO_2 turbine, but more details about flow characteristics cannot fully be displayed in Figure 6, and these will be discussed and analyzed in detail in later section.

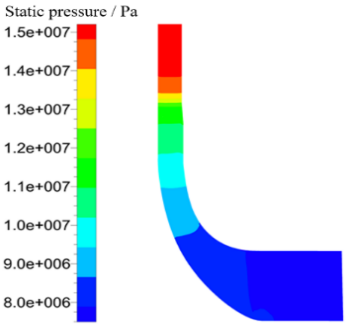

Figure 6 Static pressure distribution

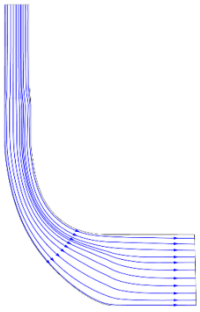

Figure 7 Streamlines in meridian passage

Figure 8 displays static pressure distribution at five span locations on the nozzle blade surface along the flow direction. From hub to shroud, pressure difference between pressure surface and suction surface is constant when horizontal coordinate value is lower than 0.9 as shown in Figure 8, which means that the variation of blade load is small enough. Because of tip clearance of impeller in existence, static pressure of the nozzle near shroud fluctuates.

In addition, static pressure and relative Mach number distribution at the mid-span are presented in Figure 9 and Figure 10. It can be seen that the flow of the working fluid is consistent with static pressure distribution, and there is no existence of the flow separation and the backflow.

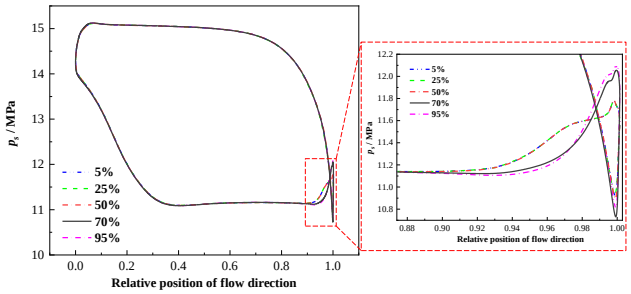

Figure 8 Static pressure distribution on the nozzle blade surface at five span locations

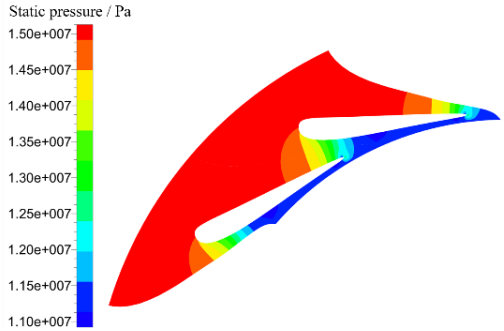

Figure 9 Static pressure at the mid-span

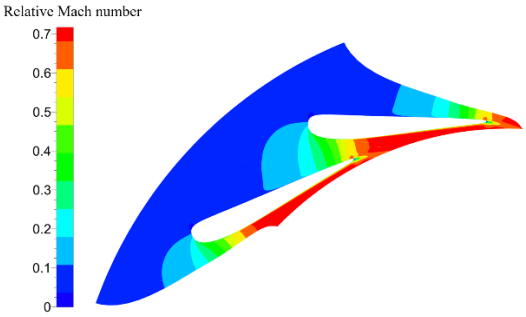

Figure 10 Relative Mach number at the mid-span

Figure 11 shows static pressure on the impeller blade surface at 10% blade height, 50% blade height and 90% blade height along the flow direction. It is found that the relatively larger adverse pressure gradient at the blade leading edge since smaller flow angle at nozzle outlet results in smaller incidence angle, which makes flow separation more serious and static pressure lower at the impeller suction surface at the same linear velocity.

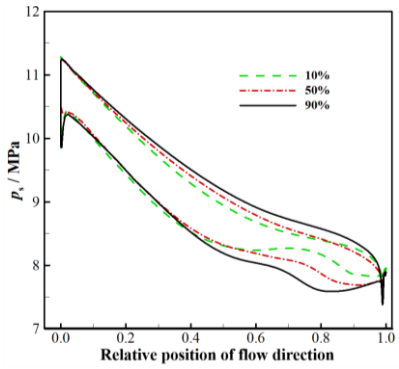

Figure 11 Static pressure distribution on impeller surface at three span locations

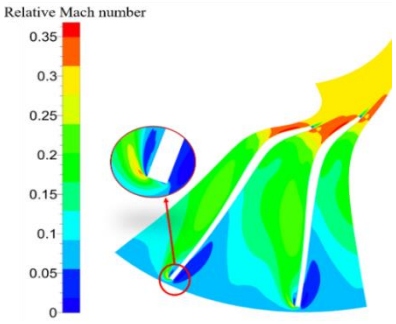

Figure 12 Relative Mach number distribution at the mid-span

The limiting streamlines of pressure surface, suction surface and endwall surface for the S-CO_2 radial inflow turbine are shown in Figure 13. Differing from flow separation observed at the leading edge shown in Figure 13(a) and Figure 13(b), flow separation occurs at the leading edge of pressure and suction surface but the separated flow will adhere quickly to the blade surface as shown in Figure 13(c). On the suction surface, the effect of Coriolis force makes separated flow adhere quickly to suction surface. On pressure surface, the main flow with high energy can impact static pressure due to the existence of negative incidence angle, which makes the low-energy separated flow reattach to the surface. In summary, flow separation has a little influence on the performances.

In Figure 13(a), it can also be clearly found that there is a separation line near blade shroud region and an attachment line near blade bub region, respectively. The separation line is formed by the scraping effect of the casing and the influence of leakage flow in shroud clearance. The scraping effect may not completely suppress the leakage flow due to greatly large relative shroud clearance about 6 %, thus a portion of the leakage flow can flow into pressure surface to interference main flow. The flow direction of the leakage flow in shroud clearance is deflected due to the influence of scraping flow resulting in vortexes in shroud region for the suction surface. Along the flow direction, the phenomenon of flow separation is more obvious because of the combined actions of weakened scraping effect and strengthened leakage flow. In addition, the attachment line on pressure surface is formed by the interaction of leakage flow from shroud clearance of the suction surface and vortexes due to negative attack angle and pressure gradient.

In Figure 13(c) where the limiting streamlines on endwall surface are presented, it can be seen that there is a saddle point at blade leading edge, and the working fluid passing through this point is divided into two streams of fluid entering turbine impeller, which indicates that horseshoe vortexes and flow separation occur at the blade leading edge. After working fluid bypassing the saddle point, the frictional force increases due to the thick boundary layer at inlet, resulting in the low-speed horseshoe vortexes cannot resist effect of centrifugal force generated by rotational impeller and the flow separation, but the streamlines of radial inflow turbine distribute uniformly. In summary, the flow characteristics meet design and operation requirements for S-CO_2 radial inflow turbine.

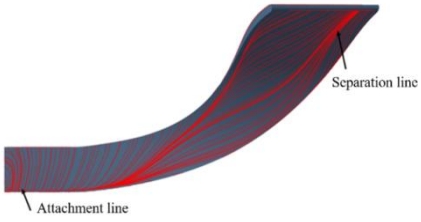

(a) Pressure surface

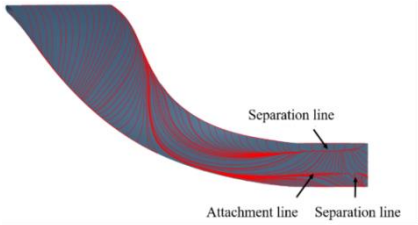

(b) Suction surface

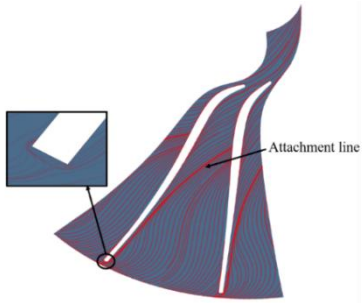

(c) Endwall surface

Figure 13 Limiting streamlines on blade surface

4.2 Performances under off design conditions

Generally, total-static efficiency of the S-CO_2 radial inflow turbine is highest under the design conditions. However, for the actual operation of S-CO_2 Brayton cycle system, the demand determines parameters of the cycle system, which results in turbine operation under the off-designed conditions. In order to provide excellent performances to the cycle system, total-static efficiency, output power and mass flow rate of the S-CO_2 turbine designed in Section 2.2 are studied by numerical method under the different working conditions.

At the time of the variation of cycle system demand, output power of the cycle system is adjusted by changing

turbine parameters such as pressure ratio and rotation speed. The variation of total-static efficiency, output power, and mass flow rate for the S-CO_2 radial inflow turbine with pressure ratio under different operated rotational speeds of 36,000, 45,000, 60,000 and 65,400 r/min are shown in Figure 14. It can be seen that total-static efficiency attains the peak at pressure ratio of 1.9 when operated rotation speed of 60,000 r/min is equal to designed that, as shown in Figure 14(a) where the trend of total-static efficiency with pressure ratio is presented. When pressure ratio ranges from 1.6 to 2.9, total-static efficiency decreases with pressure ratio increasing, but it can remain above 80 %. When pressure ratio is less than 1.6, total-static efficiency decreases rapidly to below 80 % with pressure ratio decreasing. Figure 14(b) and Figure 14(c) show the variation of output power and mass flow with pressure ratio. It can be seen that the output power and mass flow rate increase with pressure ratio increasing.

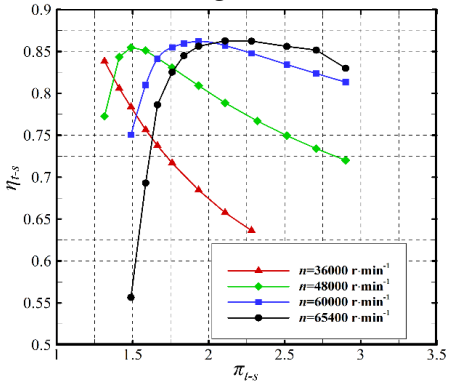

(a) Total-static efficiency

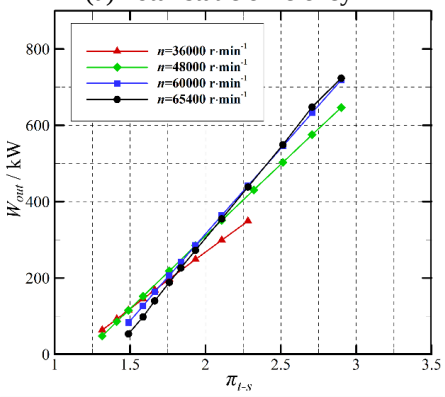

(b) Output power

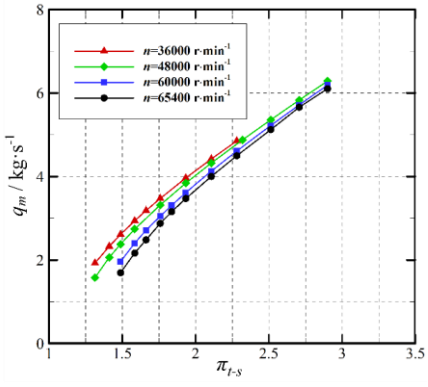

(c) Mass flow rate

Figure 14 Performances of S-CO_2 radial inflow turbine

In fact, there is a highest value of total-static efficiency at an optimal pressure ratio for a certain rotational speed, and lower operated rotational speed will make the optimal pressure ratio smaller from Figure 14(a). At the moment, it can also be found that when the operated rotational speed deviates from the designed that, total-static efficiency decreases whether the pressure ratio increases or decreases. What's more, the high efficiency region will also be more narrowed while the deviations between operated and designed rotational speed increase. In summary, the S-CO_2 radial inflow turbine designed can remain the higher operated total-static efficiency over 80 % in the wide range of operated conditions, which indicates that the turbine has excellent performances under the off-design conditions and meets the operation requirements.

5 Conclusions

In this paper, a radial inflow turbine is designed applied to 150 kW S-CO_2 Brayton cycle based on the self-programming code. In addition, flow characteristics and off-design performances are analyzed by the numerical investigation. The study results can provide the guidance for S-CO_2 radial inflow turbine design and operation. The main conclusions have been drawn as follows:

(1) The design work of thermodynamic design of S-CO_2 radial inflow turbine and three-dimensional profiled design of the nozzle and impeller blade are carried out. The thermodynamic design results are reasonable and accurate and high performances can be achieved for the S-CO_2 radial inflow turbine based on the self-programming code interlocked with REFPROP 9.0. The nozzle blade profiles are designed referring to an island nozzle, and the Non-Uniform Rational B-Splines method is used to design the impeller blade profiles. The total-static efficiency of 86% and net output power about 285.2 kW for the designed turbine can meet the design requirements of the cycle system.

(2) The flow characteristics under design condition are analyzed adopting the mesh of 1.4 million grids that can achieve grid-independent solution. The research results show the static pressure gradually decreases along the flow direction, and the obvious vortexes are generated at the shroud of the blade suction surface under the combined actions of leakage flow and scraping effect, but the streamlines of radial inflow turbine distribute uniformly. Therefore, the vortexes have little influence on the performances of the turbine, and the flow characteristics can meet design and operation requirements of S-CO_2 radial inflow turbine.

(3) The performances under off design condition are studied for the S-CO_2 radial inflow turbine. The study results show that total-static efficiency attains the peak at pressure ratio of 1.9 and operated rotation speed of 60,000 r/min, and total-static efficiency decreases with the pressure ratio increasing, but it still remains above 80 % in pressure ratio range of 1.6 ～ 2.9. What's more, output power and mass flow rate increase with the pressure ratio increasing, which indicates that the turbine has excellent performances under off-design conditions and can meet the operation requirements.

Author Contributions: Conceptualization and Writing-Original Draft Preparation, Lehao Hu;

Methodology, Yu Jiang; Software, Lehao Hu and Zhuobin Zhao; Writing-Review & Editing, Qinghua Deng, Jun Li, and Zhenping Feng.

Conflict of Interest: The authors declare that there is no conflict of interest regarding the publication of this paper.

Acknowledgments: This study is partially supported by National Key R&D Program of China (Grant No. 2017YFB0601804) and Joint Funds Key Program of the National Natural Science Foundation of China (Grant No. U20A20303).

References

[1] Angelino G. Carbon dioxide condensation cycles for power production. Journal of Engineering for Gas Turbines and Power 1968, 90: 287-295.

[2] Feher E G. The supercritical thermodynamic power cycle. Energy Conversion 1968, 8: 85-90.

[3] Cao R, Li Z G, Deng Q H, et al. Design and aerodynamic performance investigations of supercritical carbon dioxide centrifugal compressor. Proceedings of ASME Turbo Expo 2021: Turbomachinery Technical Conference and Exposition, Virtual Online, June 7-11, 2021; The American Society of Mechanical Engineers, New York, US.

[4] Xu J L, Sun E H, Li M J,et al. Key issues and solution strategies for supercritical carbon dioxide coal fired power plant. Energy 2018, 157: 227-246.

[5] Dostal V, Driscoll M J, Hejzlar P. A supercritical carbon dioxide cycle for next generation nuclear reactors; Massachusetts Institute of Technology: Cambridge, US, 2004.

[6] Bru K, Friedman P, Dennis R. Applications of supercritical carbon dioxide based power cycle; Woodhead Publishing: Duxford, UK, 2017.

[7] Wright S A. Summary of the sandia supercritical CO_2 development program supercritical carbon dioxide power cycle symposium; Sandia National Laboratory: Boulder, US, 2010.

[8] Clementoni E M, Cox T L. Practical aspects of supercritical carbon dioxide Brayton system testing. 4th International Symposium-Supercritical CO_2 Power Cycles, Pittsburgh, Pennsylvania, September 9-10, 2014; Southwest Research Institute, Texas, US.

[9] Fleming D D, Pasch J J, Conboy T M,et al. Corrosion and erosion behavior in supercritical CO_2 power cycles; Sandia National Laboratory: Boulder, US, 2011.

[10] Clementoni E M, Kimball K J. Supercritical carbon dioxide Brayton power cycle development overview. Proceedings of ASME Turbo Expo 2012: Turbomachinery Technical Conference and Exposition, Copenhagen, Denmark, June 11-15, 2012; The American Society of Mechanical Engineers, New York, US.

[11] Clementoni E M, Cox T L, Sprague C P. Startup and operation of a supercritical carbon dioxide Brayton cycle. Proceedings of ASME Turbo Expo 2013: Turbomachinery Technical Conference and Exposition, Texas, US, June 3-7, 2013; The American Society of Mechanical Engineers, New York, US.

[12] Clementoni E M, Cox T L. Steady-state power operation of a supercritical carbon dioxide Brayton cycle. Proceedings of ASME Turbo Expo 2014: Turbomachinery Technical Conference and Exposition, Düsseldorf, Germany, June 16-20, 2014; The American Society of Mechanical Engineers, New York, US.

[13] Clementoni E M, Cox T L. Comparison of carbon dioxide property measurements for an operating supercritical Brayton cycle to the Refprop physical properties database. Proceedings of ASME Turbo Expo 2014: Turbomachinery Technical Conference and Exposition, Düsseldorf, Germany, June 16-20, 2014; The American Society of Mechanical Engineers, New York, US.

[14] Cho J, Choi M, Baik Y,et al. Development of the turbomachinery for the supercritical CO_2 power cycle. International Journal of Energy Research 2015, 40: 587-599.

[15] Cho J, Shin H, Ra H S,et al. Development of the supercritical carbon dioxide power cycle experimental loop in KIER. Proceedings of ASME Turbo Expo 2016: Turbomachinery Technical Conference and Exposition, Seoul, South Korean, June 13-27, 2014; The American Society of Mechanical Engineers, New York, US.

[16] Baik Y.J, Cho J, Kim M,et al. Current R&D status of the supercritical carbon dioxide power cycle in KIER. 13th International Conference on Sustainable Energy technologies, Geneva Switzerland, August 25-28, 2014; HES-SO University, Geneva, Switzerland.

[17] Cho J, Ryong S, Minsung P,et al. Design of a small-scale supercritical carbon dioxide power cycle experimental loop. 13th International Conference on Sustainable Energy, technologies, Geneva Switzerland, August 25-28, 2014; HES-SO University, Geneva, Switzerland.

[18] Zhou A Z, Song J, Li X S,et al. Aerodynamic design and numerical analysis of a radial inflow turbine for the supercritical carbon dioxide Brayton cycle. Applied Thermal Engineering 2018, 132: 245-255.

[19] Rahual A B, Andrew M, Rajkeshar S,et al. Conceptual design of 50 MWe and 450 MWe supercritical CO_2 turbomachinery trains for power generation from coal. Part 1: Cycle and turbine. 5th International Symposium-Supercritical CO_2 Power Cycles, Texas, US, March 28-31, 2016; Southwest Research Institute, Texas, US.

[20] Rahual A B, Grant M, Day M,et al. Conceptual designs of 50MWe and 450 MWe supercritical CO_2 turbomachinery trains for power generation from coal. Part 2: Compressors. 5th International Symposium-Supercritical CO_2 Power Cycles, Texas, US, March 28-31, 2016; Southwest Research Institute, Texas, US.

[21] Wright S A, Pickard P S, Fuller R,et al. Supercritical CO_2 Brayton cycle power generation development program and initial test results. Proceedings of the ASME 2009: ASME 2009 Power Conference, New Mexico, USA. July 21-23, 2009, The American Society of Mechanical Engineers, New York, US.

[22] Balje O E, Binsley R L. Axial turbine performance evaluation Part a: loss-geometry relationship. Journal of Engineering for Power, Transaction of the ASME, 1968, 90: 341-348.

[23] Balje O E. A contribution to the problem of designing radial turbomachines, Transaction of the ASME 1952, 74: 451.

[24] Jiang Y. Comprehensive design of supercritical carbon dioxide power cycle prototype optimization system thermodynamic performance. Master Thesis, Xi'an Jiaotong University, Xi'an, 2019.

[25] Zhang H Z, Zhao H, Deng Q H,et al. Aerothermodynamic design and numerical investigation of supercritical carbon dioxide turbine. Proceedings of ASME Turbo Expo 2015: Turbomachinery Technical Conference and Exposition, Montreal, Canada, June 15-19, 2015; The American Society of Mechanical Engineers, New York, US.